A New Insight into Pyrazinamide Polymorphic Forms and their Thermodynamic Relationships

11 AUTHORS, INCLUDING:

Ricardo Castro
University of Coimbra
33 PUBLICATIONS **240** CITATIONS

SEE PROFILE

António O.L. Évora
University of Coimbra
10 PUBLICATIONS **66** CITATIONS

SEE PROFILE

João Canotilho
University of Coimbra
26 PUBLICATIONS **156** CITATIONS

SEE PROFILE

Ermelinda eusébio
University of Coimbra
47 PUBLICATIONS **255** CITATIONS

SEE PROFILE

A New Insight into Pyrazinamide Polymorphic Forms and their Thermodynamic Relationships

Ricardo A. E. Castro,[‡] Teresa M. R. Maria,[†] António O. L. Évora,[†] Joana C. Feiteira,[†] M. Ramos Silva,[#] A. Matos Beja,[#] João Canotilho,*[‡] and M. Ermelinda S. Eusébio*[†]

[†]*Department of Chemistry,* [‡]*Faculty of Pharmacy, and* [#]*CEMDRX, Department of Physics, University of Coimbra, Coimbra, Portugal*

ABSTRACT: Screening of pyrazinamide polymorphs was carried out by crystallization from solvents differing in polarity and hydrogen bonding ability and also by sublimation and lyophilization. Pure samples of polymorphs α, δ, and γ could be prepared, and mixtures of the β form with one of the other polymorphs were also produced. These forms were fully characterized by infrared spectroscopy and two main profiles registered in the N−H stretching vibration region, clearly distinguishing polymorphs encompassing a dimeric pirazinamide unit, α, β, and δ, and where the dimer does not exist, the γ one. The thermal behavior of pyrazinamide polymorphs was also investigated using differential scanning calorimetry (DSC) and polarized light thermal microscopy, supported by powder X-ray diffraction and infrared spectroscopy. The α, β, and δ forms give rise on heating to the γ form, in endothermic transitions, with some superheating being observed. Also, the DSC peaks display an irregular shape. These observations suggest kinetic hindering of the solid−solid transitions. An endothermic phase transition of the δ form to the α one was observed only for samples seeded with this latter polymorph. The relative stability of the four pyrazinamide polymorphs was derived from the experimental observations.

Introduction

Polymorphism is the ability of a compound to exist in multiple crystalline forms,[1] a common phenomenon that assumes particular relevance when active pharmaceutical ingredients are involved. The increasing recognition of the importance of polymorphism to the life sciences industry has generated a great deal of interest and the field has been evolving rapidly. In fact, the systematic evaluation and characterization of polymorphic forms of drugs is essential and mandatory, because important properties such as solubility and drug stability depend on the solid state structure.[2−4]

Pyrazinamide, pyrazine-2-carboxamide, Figure 1, is one of the first-line drugs in antituberculosis treatment,[5−7] recommended by the World Health Organization.[8]

Pyrazinamide molecule is rather rigid: only two relevant conformers, having quite different energies, have been identified in the gas phase.[9,10] Therefore, in opposition to more flexible molecules, no conformational polymorphism is to be expected.[11,12] On the other hand, the different possibilities of intermolecular hydrogen bonds may promote the occurrence of packing polymorphism. As a matter of fact, four packing polymorphic pyrazinamide forms have already been identified, α, β, γ, and δ, as well as a possible fifth polymorph, α′, similar to α,[13−21] although no information on their thermal behavior and relative phase stability is available. Similar melting point values are reported for all forms.[13,16−18,22]

In the present work screening of pyrazinamide polymorphic forms is performed, and the solids obtained were characterized by X-ray diffraction, infrared spectroscopy, and thermal analysis. Their thermal behavior and relative phase stability are investigated.
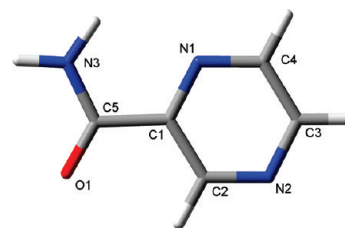

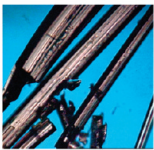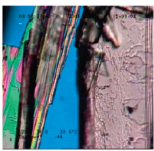**Figure 1.** Pyrazinamide molecular structure and atom numbering.
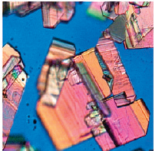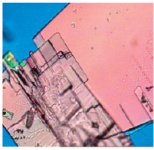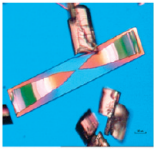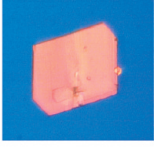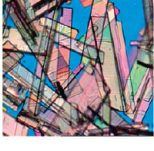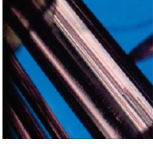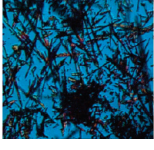
Experimental Procedures

Polymorph Screening. Pyrazinamide was acquired from Fluka, with specified purity greater than 99% (N). In the screening of pyrazinamide polymorphic forms, different crystallization processes and conditions were employed. In procedure 1, P1, ~0.05 mmol of the original material was dissolved in 6 mL of a reagent grade solvent, at room temperature, the solutions filtered to a Petri dish, and the solvent was evaporated at room temperature (ca. 20 °C). Different solvents were used and the solids obtained were analyzed typically after a two week period. In procedure 2, P2, solutions were prepared as in P1, and after filtration they were transferred to a refrigerator at 4 °C, and the solvent was evaporated at this temperature. A pure pyrazinamide polymorph was obtained by sublimation (procedure 3, P3) carried out at atmospheric pressure from a stainless steel cylindrical cell (1 cm diameter, 1 cm height), whose metallic cover has an orifice (3 mm diameter). Crystals were collected in a glass slide positioned over the cell cover when the set was heated up to $T \sim 142$ °C. The fourth procedure assayed, P4, consisted in a lyophilization process carried out in a Labconco freeze-dryer, model 79480. Twenty-five milliliters of an aqueous pyrazinamide solution (0.4% w/v) were placed in a 100 mL vial, cooled to −80 °C and held at that temperature for 1 h. Drying was carried out at $p = 0.08$ mbar, using the following protocol: −30 °C (2 h), −10 °C (4 h), 0 °C (6 h), 10 °C (48 h). Afterward, the shelf temperature was increased to 25 °C to complete drying at the same pressure.
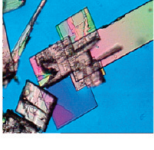
Single-Crystal X-ray Diffraction (SXD). The analysis of a small crystal of the γ polymorph was made on a Bruker-Nonius Kappa

*To whom correspondence should be addressed. E-mail: quierme@ci.uc.pt (M.E.S.E.); jcano@ci.uc.pt (J.C.).

Table 1. Examples (16/60) of Pyrazinamide Forms Obtained in the Screening Process

#	Crystal habit (200x)	Solvent / Crystallization process / Polymorphic form	#	Crystal habit (200x)	Solvent / Crystallization process / Polymorphic form
1		Water / P1 / α	9		Methanol / P2 / δ
2		Water / ethanol (1:1, V/V) / P1 / α	10		Acetone / P2 / δ
3		THF / P1 / δ	11		Acetic acid / P2 / δ
4		Dioxane / P1 / β, γ	12		Acetonitrile / P2 / α, δ
5		Toluene / ethanol (1:1, V/V) / P1 / δ, γ	13		THF / P2 / δ
6		Nitromethane / P1 / δ	14		Chloroform / P2 / β, δ
7		Dichloromethane / P1 / β, δ	15		P3 / γ
8		Water / P2 / α	16		P4 / γ

Apex II CCD diffractometer using graphite monochromated Mo $K\alpha$ radiation ($\lambda = 0.71073$ Å). The structures were solved by direct methods and conventional Fourier synthesis (SHELXS-97). The refinement of the structures was made by full matrix least-squares on F^2 (SHELXL-97). All non-H-atoms were refined anisotropically. The

H atoms positions were initially placed at idealized calculated positions and refined with isotropic thermal factors while allowed to ride on the attached parent atoms using SHELXL-97 defaults. Because of the absence of strong anomalous scatterers at Mo $K\alpha$ wavelength, the Friedel pairs were merged in the last cycles of the refinement.

X-ray Powder Diffraction (XRPD). A glass capillary was filled with the powder obtained by grinding the solids. The samples were mounted on an ENRAF-NONIUS powder diffractometer (equipped with a CPS120 detector by INEL) and data were collected for 5 h using Debye−Scherrer geometry. Cu Kα_1 radiation was used (λ = 1.540598 Å). Potassium aluminum sulfate dodecahydrate was chosen as an external calibrant.

Infrared Spectroscopy (FTIR). Spectra of the solids were recorded at room temperature in a FTIR spectrometer, ThermoNicolet IR300, resolution 1 cm^{-1}, using the KBr pellet technique and in a PerkinElmer Spectrum 400 FTIR/ATR, resolution 1 cm^{-1}.

Polarized Light Thermal Microscopy (PLTM). The solids obtained were characterized by PLTM using a hot stage Linkam system, model DSC600, with a Leica DMRB microscope and a Sony CCD-IRIS/RGB video camera. Real Time Video Measurement System software by Linkam was used for image analysis. The images were obtained by the combined use of polarized light and wave compensators, using a 200× magnification.

Differential Scanning Calorimetry (DSC). The studies were performed in a Pyris1 power compensation calorimeter from Perkin-Elmer, with an intracooler cooling unit at −10 °C (ethylenglycol−water, 1:1, cooling mixture). The samples were hermetically sealed in aluminum pans and as reference an empty pan was used. A 20 mL/min nitrogen purge was employed. Temperature calibration[23,24] was performed with high grade standards, namely, biphenyl (CRM LGC 2610, T_{fus} = 68.93 ± 0.03 °C), benzoic acid (CRM LGC 2606, T_{fus} = 122.35 ± 0.02 °C), indium (Perkin-Elmer, x = 99.99%, T_{fus} = 156.60 °C), and caffeine (Mettler Toledo calibration substance, ME 18 872, T_{fus} = 235.6 ± 0.2 °C). Enthalpy calibration was performed with indium ($\Delta_{fus}H$ = 3286 ± 13 J/mol).[23] In typical DSC or PLTM experiments, the sample was scanned from 25 to 197 °C at a 10 °C/min heating rate.

Results and Discussion

Polymorph Screening. Some solid forms obtained by crystallization from solutions, sublimation and lyophilization are presented in Table 1. These materials were characterized by the similarity between the XRPD and the simulated spectra of the already known pyrazinamide polymorphs. Figure 2 show this comparison for the commercial compound, identified as polymorph α (2θ = 7.8, 13.7, 15.3, 17.7, 24.3, 26.4, 27.4, 27.6, 27.8), and the outcomes of experiment #10, δ polymorph (main 2θ = 9.1, 16.4, 17.3, 18.2, 20.0, 23.5, 27.7), experiment #16, γ form (main 2θ = 12.9, 17.3, 18.4, 23.9, 25.4, 25.9, 27.2, 27.4, 29.7, 30.3, 33.6, 39.3) and experiment #4, a mixture of β (main 2θ = 12.6, 16.8, 16.9, 25.3, 25.5, 26.7, 27.2) and γ polymorphs. It is concluded that no new crystalline form could be identified.

Single crystals of forms α, β, δ, and γ could be obtained, respectively, from water (#1), dioxane (#4), methanol (#9), and by sublimation (#15).

As it is evident from Table 1, pure α, δ, and γ polymorphs could be obtained by different crystallization processes and conditions. β form is concomitant with δ or γ polymorphs. Therefore, a complete infrared spectral characterization of these forms and thermal behavior study can be undertaken.

Single-Crystal X-ray Diffraction (SXD). Two entries[16,20] already exist in the Cambridge Structural Database concerning the γ polymorph, but none of them contained the coordinates of all atoms. The analysis of a small crystal of this polymorph, obtained by sublimation, gave rise to the following crystallographic data: $C_5H_5N_3O_1$, M = 123.13, crystal dimensions 0.27 × 0.12 × 0.09 mm^3, monoclinic, Pc, a = 7.1830(4) Å, b = 3.7291(2) Å, c = 10.7581(5) Å, α = 90°, β = 106.767(2) °, γ = 90°, V = 275.92(2) Å^3, Z = 2, ρ_{calc} = 1.482 g cm^{-3}, 6789 reflections measured, 554 independent, R = 0.1066 (506 reflections with $I > 2\sigma(I)$), R_w = 0.2978 for all reflections, GOF = 1.098, 82 parameters,
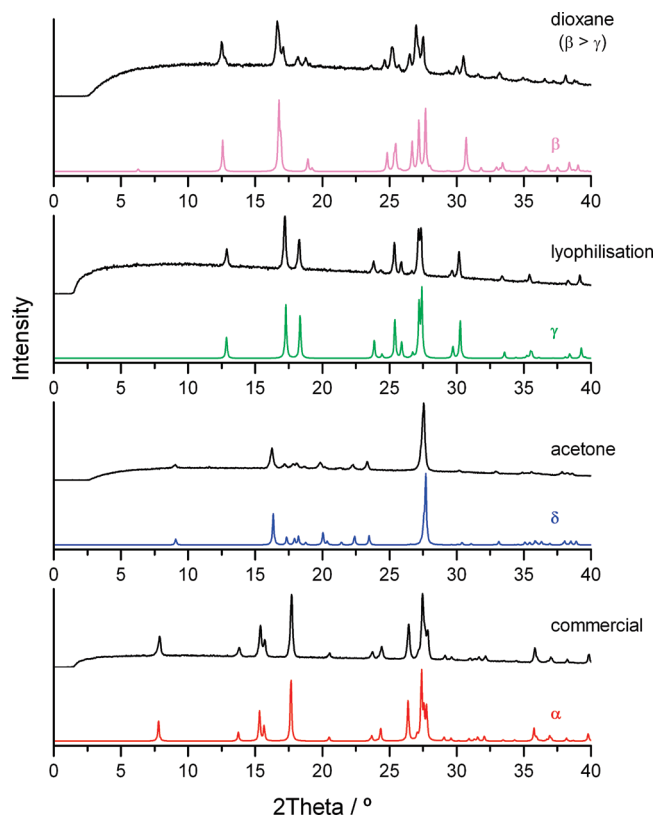

Figure 2. Experimental (up) and simulated (down) XRPD of pyrazinamide: α form,[13] commercial; δ form,[18] acetone (#10); γ form,[20] lyophilization (#16); mixture of β form[17] and γ form, dioxane (#4).

residual density 0.883/−0.286 e Å^{-3}. The fractional atomic coordinates and equivalent isotropic displacement parameters as well as other crystallographic data have been deposited at the Cambridge Crystallographic Data Centre (CCDC 754512).

Concerning the packing of the molecules in the different polymorphs, striking differences can be seen, Figure 3. In the α polymorph, the molecules are linked in centrosymmetric planar dimers that aggregate other dimers sideways forming planar ribbons. Neighboring ribbons are joined by C−H···N interactions, but the ribbons do not share the same plane. In the β polymorph, there is again the formation of centrosymmetric planar dimers that aggregate other dimers side-to-side. To allow a better approximation of the dimers, the planes of consecutive dimers make an angle of 49.5°. The δ polymorph shows also the molecules linked in pairs with the same head-to-head approximation. Contrary to the former polymorphs, the dimers do not aggregate any molecule sideways but form planar chains through C−H···N interactions. The chains assemble in layers. In the γ polymorph the molecules assemble head-to-tail with each molecule making an angle of 49.3(9)° with its closest neighbors. Although in the β polymorph the molecules are joined in head-to-head dimers and in the γ polymorph the molecules are head to tail, these two structures have similar spatial arrangements, and such similarity is reflected in the similar cell parameters (see Table S1, Supporting Information, for a summary of crystallographic data of pyrazinamide polymorphs).

Infrared Spectral Characterization. Some previous work exists aiming at[9,25−29] or including[30,31] the infrared spectral

characterization of solid pyrazinamide. However, in most of these works the polymorphic form investigated is not identified, as in refs 9, 25−27, and 30; in two of them the α-form was used[29,31] and in the Yoshida paper[28] a α-type pyrazinamide, possessing a dimeric unit, and a β-type one are referred to with no X-ray diffraction supporting data.
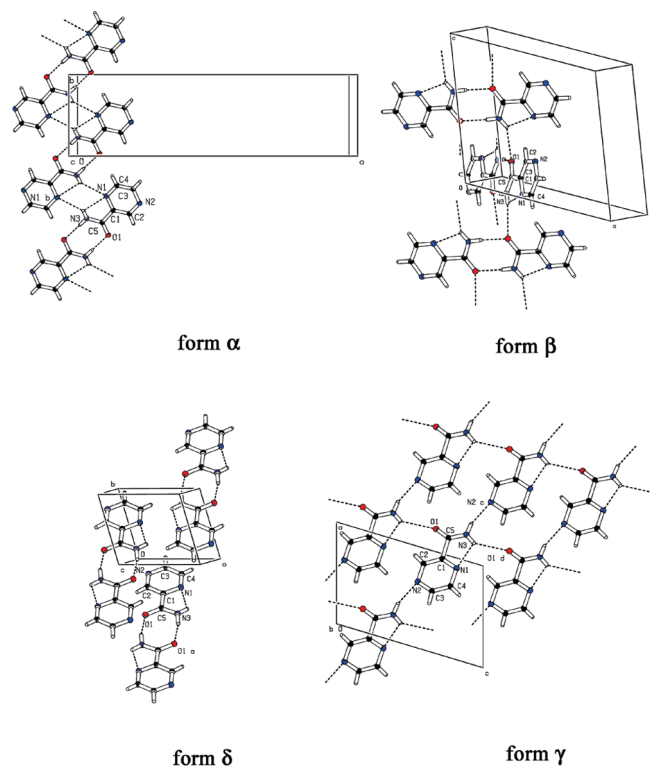
It is possible from our results to go a step forward in the infrared spectral characterization of pyrazinamide solid forms given that pure α, δ, and γ polymorphs could be produced.

Infrared spectra of the different specimens were first obtained in an FTIR/ATR spectrometer in order to minimize the solid samples manipulation. As no polymorph changes were induced by grinding on KBr pellets preparation, the spectra presented in this paper are those obtained by this technique.

Infrared spectra of the pyrazinamide polymorphs α, δ, and γ are presented in Figure 4, as well as the spectrum of the mixture of the β and γ forms obtained in dioxane. In Table 2 the wavenumbers corresponding to the main bands are shown and a tentative assignment carried out, based on the experimental works of Yoshida[28] and Delgado et al.[29] and on theoretical calculations by Chiş et al.[9] and Borba et al.[10]

Figure 3. Pyrazinamide polymorphic forms: α form;[13] β form;[17] δ form;[18] γ form.
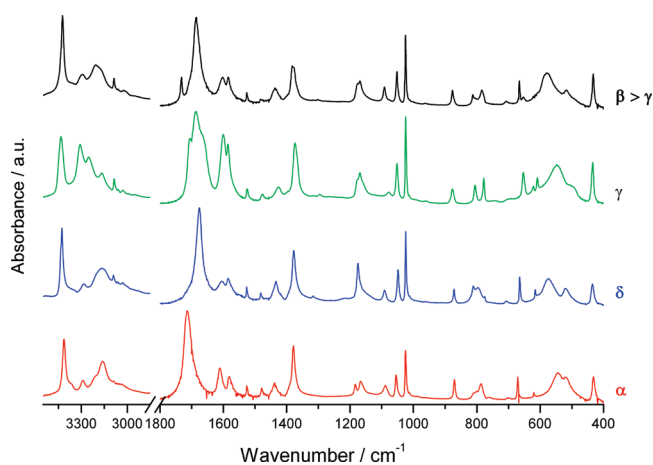

Figure 4. Infrared spectra of α, δ, and γ pyrazinamide polymorphs and of a mixture of β and γ forms.

Table 2. Experimental Infrared Spectra of Pyrazinamide α, δ, and γ Polymorphs at Ambient Temperature and Tentative Band Assignment

$\bar{\nu}$ / cm^{-1}			Tentative Assignment[a]
Form α	Form δ	Form γ	
3412	3426	3433	$\nu_{ass}(NH_2)$
3364(sh); 3291	3284	3309	$\nu_s(NH_2)$
		3250	$\nu(NH_2)$
3211(sh); 3163	3169	3165	$\nu_s(NH_2)$
3086	3089	3086	$\nu(CH)$
1714	1676	1707(sh);1686;1665(sh)	$\nu(C=O) + \delta(NH_2)$ Amide I
1611	1605	1600	$\delta(NH_2)$ Amide II
1582	1585	1585	
1525	1525	1524	
1479	1481	1476	Ring vibrations
1438	1434	1425	
1379	1378	1373	$\nu(C-N)$ Amide III
	1316	1296	
1184; 1166	1175(sh)	1177(sh); 1169	$\rho(NH_2) + \nu(C-N) + \nu(C-C)$ ring $+ \delta(CH)$
1088	1090	1076	$\rho(NH_2)$
1054	1048	1052	δ ring
1024	1024	1024	δ ring
870	870	876	$\gamma(C-H)$
810(sh);801(sh); 787	811;796;776	805; 778	δ ring, τ ring
670	666	654	δ ring
620	616	622;609	τ ring
544; 520	575; 521	548; 508(sh)	ring bending $+ \rho(NH_2)$
432	435	433	ring bending

ν – stretching; δ – in plane bending; ρ- rocking; γ – out of plane bending; τ- torsion; sh- shoulder.

[a] Assignment based on refs.[9, 10, 28, 29]

Table 3. Hydrogen Bond Parameters in Pyrazinamide Polymorphs[13,17,18]

type	D−H⋯A	D⋯A/Å	H⋯A/Å	D−H⋯A/°	symmetry code
		α			
intra	N3−H3′⋯N1	2.720	2.37	104	
	N3−H3′⋯N1^i	3.138	2.46	136	i: $-x, -1-y, -1-z$
	N3−H3⋯O1^{ii}	2.905	2.03	179	ii: $-x, -2-y, -2-z$
		β			
intra	N3−H3′⋯N1	2.735	2.39	106	
	N3−H3′⋯O1^i	3.242	2.53	146	i: $-x, 2-y, -z$
	N3−H3⋯O1^{ii}	2.923	1.99	168	ii: $x, 3/2-y, -1/2+z$
		δ			
intra	N3−H3′⋯N1	2.733	2.26	115	
	N3−H3⋯O1^i	2.897	1.90	167	i: $-x, -2-y, -z$
		γ			
intra	N3−H3′⋯N1	2.62	2.21	109	
	N3−H3⋯N2^i	3.09	2.26	162	i: $1-x, 2-y, 1/2+z$
	N3−H3′⋯O1^{ii}	3.25	2.57	136	ii: $x, 2-z, 1/2+z$

The infrared spectra of the different polymorphs allow a clear identification of the distinct solid forms. Using our data it can be concluded that α polymorph was the one investigated by Chiş,[9] Akyuz,[30] Favila,[26] and Gunasekaran.[27] Yoshida[28] studied the α (his α-type specimen) and the γ (his β-type one) polymorphs. The identification of the solid form used by Kalkar[25] is not straightforward; it seems that a mixture of forms was studied.

Infrared spectra are quite sensitive to the hydrogen bond network present in the specimens analyzed. In what concerns pyrazinamide polymorphs in the α, β, and δ forms two molecules join together forming a dimeric unit linked by N3−H3⋯O1 hydrogen bond interactions (see Figure 3 and Table 3). Forms α and β have an additional weaker H-bond between N3−H3′⋯N1 and N3−H3′⋯O1, respectively. The γ polymorph has a quite different hydrogen bond pattern: the dimer does not exist, and each molecule is linked to two others (N3−H3⋯N2 and N3−H3′⋯O1) forming strong to weak hydrogen bonds.[32] In all forms, a weak intramolecular hydrogen bond also exists between the amide group and N1.

The main differences observed among the spectra of pyrazinamide polymorphs rely on the bands associated with the amide group, as expected due to the different hydrogen bond patterns involving this group that can be found in the forms. In fact, clear differences are observed in the NH stretching bands (between ~3450 and 3150 cm^{-1}), in the amide I region, with combined contributions of the C=O stretching vibration and of the NH$_2$ in plane bending (~1714 to 1660 cm^{-1}), in the amide II region (1611 to 1600 cm^{-1}), in the bands with a contribution from the NH$_2$ rock vibration (around 1180 and 1080 cm^{-1}). Significant differences are also observed for bands centered at around 800 and 550 cm^{-1} attributed to ring vibrations.

In the NH stretching region, besides the differences in the band maxima wavenumber values, it is worth noting that the spectral pattern clearly distinguishes the polymorphs having a dimeric pyrazinamide unit, the α, β, and δ forms, from the γ polymorph in which the dimer does not exist. The spectrum of β + γ mixture reflects, as already shown in XRPD, the predominance of the β form.

In the amide I region the bands observed for the α and δ polymorphs have relatively simple patterns, and once again the γ form presents a different (and in this case a more complex) pattern. The δ form, with stronger hydrogen bonds, has the lower frequency maximum 1676 cm^{-1}. The β and γ mixture shows two bands in the amide I region. The 1730 cm^{-1} band can be ascribed to the β polymorph, and may be associated to the weaker hydrogen bond, N3−H3′⋯O1, involving the carbonyl group.

Thermal Analysis Study. A combined DSC and polarized light thermomicroscopy study was performed on different pyrazinamide specimens, in order to characterize their thermal behavior from ambient temperature until fusion. Representative DSC curves of heating runs performed at a 10 °C/min scanning rate are presented in Figure 5a for the α polymorph (the commercial compound), the γ polymorph (#16, lyophilized sample), and the δ polymorph obtained from acetone, #10 and from tetrahydrofuran, #13. Table 4 shows the thermodynamic data of the observed phase transitions.

Polymorphs α and δ undergo solid−solid phase transitions upon heating, as confirmed by PLTM (Figure 5b), whose enthalpies are low. For the γ polymorph, no phase transition but fusion is observed.

Pyrazinamide α-polymorph was ascribed a melting temperature value between 188 and 193 °C[13,22] and the δ form 188 °C.[22] However, even at a 50 °C/min heating rate the solid−solid transitions could not be prevented and the melting processes of polymorphs α or δ were not observed. Moreover, for all the specimens investigated the solid−solid transformations are not reversed either on cooling runs carried out at rates as low as 1 °C/min rate or on standing at room temperature for the investigated period of one month (the typical behavior is exemplified in Figure 6, for polymorph α).

A pyrazinamide sample prepared by heating the α polymorph up to 165 °C, in a DSC pan, and cooling to room temperature, was analyzed by XRPD and FTIR/ATR. From the results obtained, it is concluded that, in the heating process, pyrazinamide α polymorph transforms into polymorph γ, which melts at T = 188 °C. Identical results were obtained for the δ polymorph, crystallized from tetrahydrofuran, submitted to the same thermal treatment and also, as expected, for the δ polymorph obtained from acetone, upon heating to 137 °C, and cooling to room temperature.

The kinetic constraints of the δ → γ transition are clearly evident from the results obtained for the δ form crystallized from acetone or from tetrahydrofuran: the transition temperature depends on the solid morphology and superheating is observed. This last observation was further confirmed
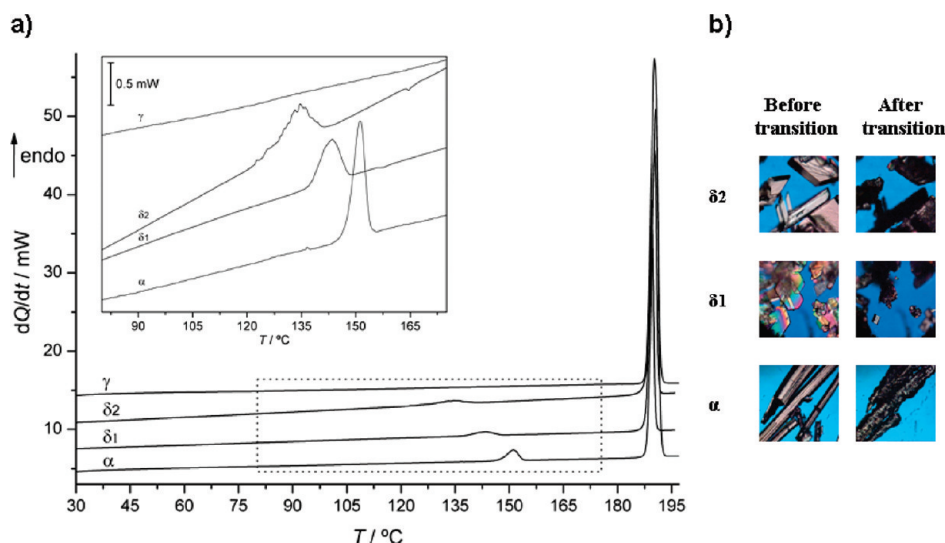
Figure 5. (a) DSC heating curves of pyrazinamide: α (commercial), δ1 (THF, #13), δ2 (acetone, #10) and γ (lyophilized, #16); scanning rate 10 °C/min; (b) PLTM images recorded before and after the solid−solid transitions in #10, #13, #1.

Table 4. Thermodynamic Parameters of α, δ, and γ Pyrazinamide Polymorphs Phase Transitions (Studied between 25 °C and Fusion, Scanning Rate 10 °C/min)

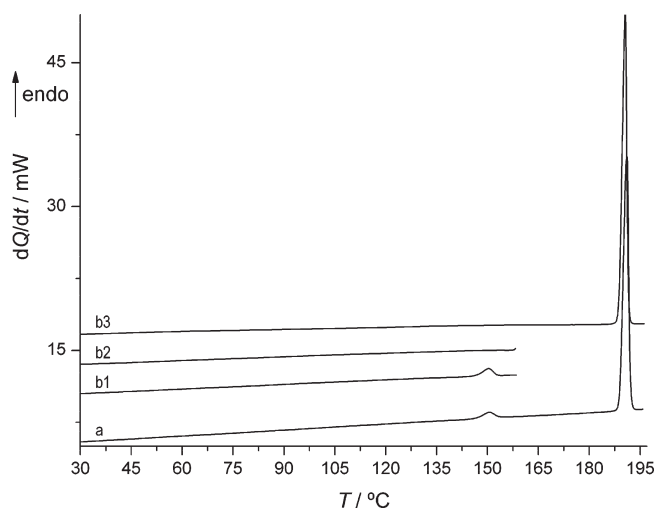|	peak 1		peak 2	
sample	T / °C	ΔH / kJ/mol	T / °C	ΔH / kJ/mol
α commercial	146.9 ± 0.5 ($n = 9$)	1.63 ± 0.08 ($n = 9$)	188.3 ± 0.1 ($n = 6$)	28.1 ± 0.3 ($n = 6$)
γ lyophilized, #16			187.9 ± 0.5 ($n = 6$)	28.1 ± 0.5 ($n = 6$)
δ THF, #13	138.1 ± 0.8 ($n = 5$)	2.05 ± 0.05 ($n = 5$)	188.3 ± 0.1 ($n = 5$)	28.3 ± 0.3 ($n = 5$)
δ acetone, #10	131.6 ± 0.8 ($n = 4$)	2.1 ± 0.2 ($n = 4$)	188.4 ± 0.2 ($n = 6$)	28.0 ± 0.4 ($n = 6$)

Figure 6. a DSC heating curve of polymorph α, between 25 and 197 °C, $m = 1.29$ mg; **b1** DSC heating curve of polymorph α, between 25 and 160 °C, $m = 1.38$ mg; **b2** cooling run following **b1**; **b3** heating run performed one month after **b2**. Scanning rate 10 °C/min.

from heating scans at lower rates, namely, 5, 2, and 0.5 °C/min: the solid−solid phase transition occurs at lower temperature for lower heating rate (acetone crystallized δ form $T_{trs} = 129.2$ at 5 °C/min, $T_{trs} = 127.1$ at 2 °C/min and $T_{trs} = 125.3$ at 0.5 °C/min). The same observation could be made on
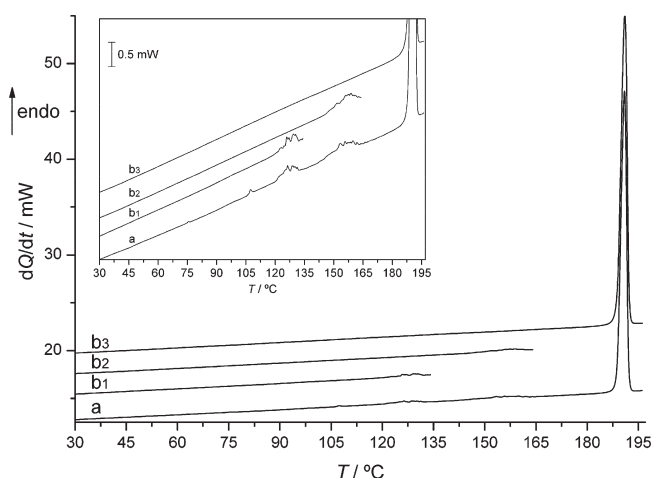

Figure 7. DSC heating curves of pyrazinamide crystallized from acetonitrile, #12, polymorphs α and δ. **a** $m = 1.61$ mg, 25 °C → 197 °C; **b1** $m = 1.81$ mg, 25 °C → 135 °C; **b2** 25 °C → 165 °C after cooling **b1** to 25 °C; **b3** 25 °C → 197 °C after cooling **b2** to 25 °C. Scanning rate 10 °C/min.

the commercial α form: at a 5 °C/min heating rate $T_{trs} = 145.1$ °C, at 2 °C/min $T_{trs} = 141.2$ °C and at 0.5 °C/min a value of $T_{trs} = 139.7$ °C was found (See Figure S1, Supporting Information, for the effect of the heating rate on the α → γ and on the δ→γ transition temperatures). This behavior indicates that the solid−solid transitions are kinetically hindered.[33,34] In all cases, as expected, the melting temperature is independent of the heating rate. Taking into account the structural X-ray information it is evident that the transformation of any of the polymorphs into the γ phase requires a rotation of 180° of half the molecules, which may justify the kinetic constraints observed.

The relative stability of α and δ polymorphs was investigated from the mixture of these forms obtained from acetonitrile (#12). The DSC heating curves of this specimen are presented in Figure 7. Two endothermic transitions are observed before the melting peak. The phase transformations that take place on heating could be followed by FTIR, as the solid−solid transitions are kinetically inhibited on cooling, in the experimental conditions employed. FTIR
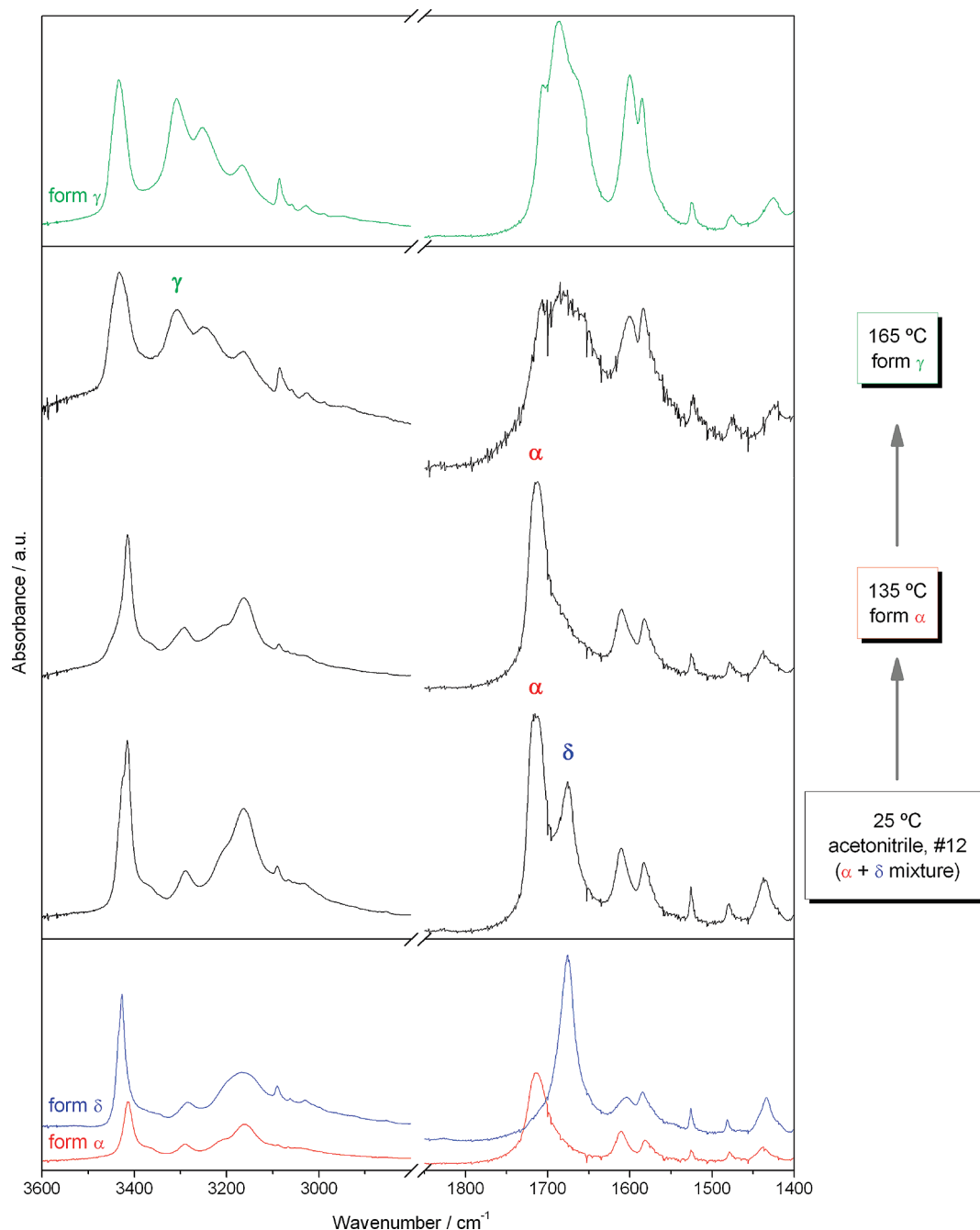
Figure 8. Infrared spectra collected at 25 °C. Samples of pyrazinamide crystallized from acetonitrile, #12, concomitant polymorphs α and δ, were heated to 135 and 165 °C. Reference spectra of α and δ (down) and γ (up).

spectra of the original sample, Figure 8, confirms the presence of both α and δ polymorphs; spectra were also collected for a sample heated to 135 °C (as in DSC curve b1, Figure 7) and cooled to ambient temperature, and finally for a sample heated to 165 °C. It is evident from Figure 8 that polymorph δ transitions to form α, which then changes to the γ solid form. The identity of the solid phases was further confirmed by XRPD experiments, performed on samples prepared in a similar way.

The δ → α transition occurs at T = (122 ± 1) °C, at a 10 °C/min scanning rate (as determined by DSC experiments on the acetonitrile sample and on a pure δ polymorph - acetone crystallized - doped with pure α form). As can be seen in Figure 7 the solid−solid transition peaks have an irregular shape, which is ascribed to the kinetic hindering of

the transitions and to the lack of homogeneity of individual crystals.[35]

Although the pure β form could not be obtained, DSC and PLTM experiments performed on the (β + γ) mixture #4, Figure 9, show a solid/solid endothermic transition around 95 °C originating the γ polymorph, as confirmed by FTIR.

Figure 10 summarizes all the phase transformations observed in the present study. All these phase transitions are endothermic, and in the absence of significant conformational changes of the pyrazinamide molecule in the different polymorphs, this behavior indicates an enantiotropic relationship between the phases involved.[36−38] According to Burger and Ramberger, this heat transition rule makes correct predictions in 99% of the cases.[37] From the thermal behavior study of pyrazinamide forms α, β, δ, and γ, the
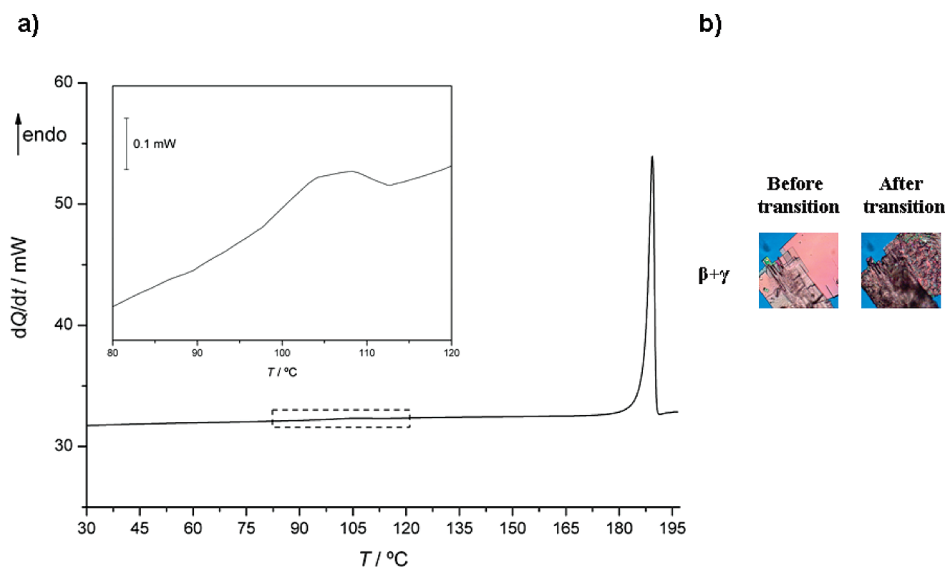
a)

b)

Figure 9. (a) DSC heating curves of pyrazinamide crystallized from dioxane, #4, polymorphs β and γ. $m = 1.66$ mg. Scanning rate 10 °C/min. (b) PLTM images recorded before and after the solid−solid transition.
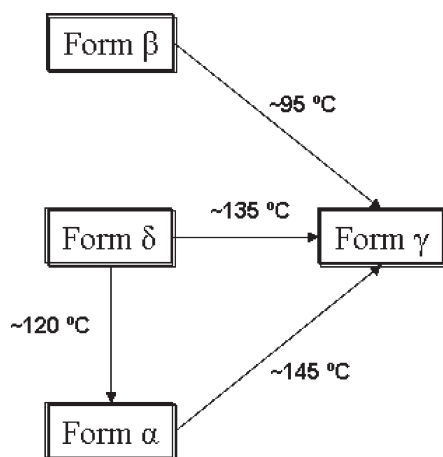

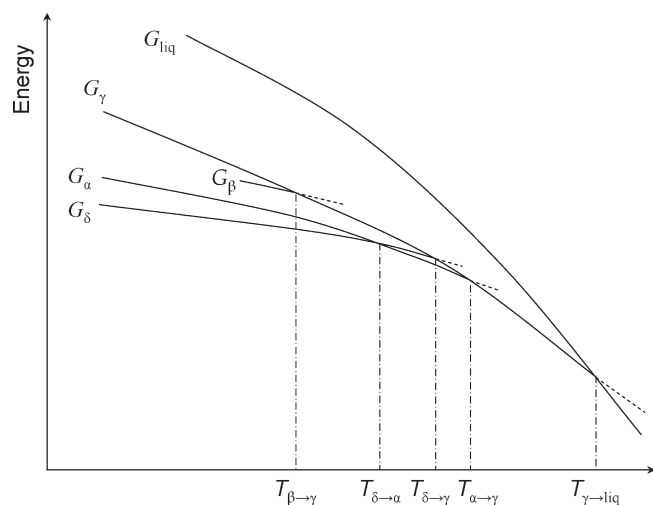**Figure 10.** Interconversion of the different polymorphic forms of pirazynamide (scanning rate 10 °C/min).

Figure 11. Energy/temperature diagram of the crystalline forms (α, β, δ, and γ) of pyrazinamide: G, free energy; T, transition temperature, liq, liquid.

Gibbs energy- temperature diagram presented in Figure 11 may be envisaged.

Conclusions

Reproducible strategies to obtain pure pyrazinamide α, δ, and γ polymorphs were developed. For the first time, a full infrared spectral characterization of these forms as well as the investigation of their thermal behavior was undertaken.

The infrared spectra exhibit two main profiles in the N−H stretching vibration region, clearly distinguishing the polymorphs α, β, and δ, whose crystalline structures have pyrazinamide dimers, from the γ one. Furthermore, significant differences between polymorphs exists in the $\nu(C{=}O) + \delta(NH_2)$, $\rho(NH_2)$ and in ring vibration modes centered at around 800 and 550 cm^{-1}.

The thermal analysis study demonstrated an interesting scheme of solid phases interconversion. Solid−solid endothermic phase transitions giving rise to the γ form are observed for the three polymorphs having pyrazinamide dimeric units, being the γ polymorph the stable phase for temperature values higher than ~145 °C. An endothermic phase transition of the δ form to the α one was observed for samples seeded with this last polymorph. Kinetic hindering of the solid−solid transitions was observed both in the heating and in the cooling runs.

This study allows us to establish the relative stability of the different polymorphic forms of pyrazinamide. A diagram of energy/temperature is proposed.

Supporting Information Available: Table S1 and Figure S1. This information is available free of charge via the Internet at http://pubs.acs.org.

References

(1) McCrone, W. C. Physics and chemistry of the organic solid state. In *Polymorphism*; Fox, D.; Labes, M. M.; Weissberger, A., Eds.; Wiley Interscience: New York, 1965; Vol. 2, pp 725−767.

(2) Brittain, H. G. *Polymorphism in Pharmaceutical Solids*; Marcel Dekker, Inc.: New York, 1999.

(3) Bernstein, J. *Polymorphism in Molecular Crystals*; Oxford Science Publications: Oxford, 2002.

(4) Hilfiker, R. *Polymorphism in the Pharmaceutical Industry*; Wiley-VCH: Weinheim, 2006; pp 1−19.

(5) Chopra, I.; Brennan, P. *Tuber. Lung Dis.* **1998**, *78*, 89–98.

(6) Dessen, A.; Quemard, A.; Blanchard, J. S.; Jacobs, W. R.; Sacchettini, J. C. *Science* **1995**, *267*, 1638–1641.

(7) Somoskovi, A.; Wade, M. M.; Sun, Z. H.; Zhang, Y. *J. Antimicrob. Chemother.* **2004**, *53*, 192–196.

(8) Maher, D.; Chaulet, P.; Spinaci, S.; Harries, A. *Treatment of tuberculosis: Guidelines for national programmes*; World Health Organization: Geneva, 1997.

(9) Chis, V.; Pirnau, A.; Jurca, T.; Vasilescu, M.; Simon, S.; Cozar, O.; David, L. *Chem. Phys.* **2005**, *316*, 153–163.

(10) Borba, A.; Albrecht, M.; Gómez-Zavaglia, A.; Suhm, M. A.; Fausto, R. *J. Phys. Chem. A* **2009**, DOI: 10.1021/jp907466h.

(11) Castro, R. A. E.; Canotilho, J.; Barbosa, R. M.; Silva, M. R.; Beja, A. M.; Paixao, J. A.; Redinha, J. S. *Cryst. Growth Des.* **2007**, *7*, 496–500.

(12) Nangia, A. *Acc. Chem. Res.* **2008**, *41*, 595–604.

(13) Takaki, Y.; Sasada, Y.; Watanabe, T. *Acta Crystallogr.* **1960**, *13*, 693–702.

(14) Tiwari, R. K.; Patel, T. C.; Singh, T. P. *Indian J. Phys., A* **1982**, *56*, 413–419.

(15) Nangia, A.; Srinivasulu, A. *Private Communication, CCDC-PYR-ZIN15*, **2005**.

(16) Tamura, C.; Sasada, Y.; Kuwano, H. *Acta Crystallogr.* **1961**, *14*, 693–694.

(17) Ro, G.; Sorum, H. *Acta Crystallogr., Sect. B: Struct. Sci.* **1972**, *B 28*, 991–998.

(18) Ro, G.; Sorum, H. *Acta Crystallogr., Sect. B: Struct. Sci.* **1972**, *B 28*, 1677–1684.

(19) Nangia, A.; Srinivasulu, A. *Private Communication, CCDC-PYR-ZIN16* **2005**.

(20) Nakata, K.; Takaki, Y. *Mem. Osaka Kyoiku Univ. Ser. III* **1987**, *36*, 93–97.

(21) Nangia, A.; Desiraju, G. R. *Top. Curr. Chem.* **1998**, *198*, 57–96.

(22) Felder, E.; Pitre, D. *Analytical Profiles of Drug Substances and Excipients: Pyrazinamide*; Academic Press: San Diego, CA., 1979; Vol. 12, pp 433−462.

(23) Sabbah, R.; An, X. W.; Chickos, J. S.; Leitao, M. L. P.; Roux, M. V.; Torres, L. A. *Thermochim. Acta* **1999**, *331*, 93–204.

(24) Della Gatta, G.; Richardson, M. J.; Sarge, S. M.; Stolen, S. *Pure Appl. Chem.* **2006**, *78*, 1455–1476.

(25) Kalkar, A. K.; Bhosekar, N. M.; Kshirsagar, S. T. *Spectrochim. Acta, Part A* **1989**, *45*, 635–641.

(26) Favila, A.; Gallo, M.; Glossman-Mitnik, D. *J. Mol. Modeling* **2007**, *13*, 505–518.

(27) Gunasekaran, S.; Sailatha, E. *Indian J. Pure Appl. Phys.* **2009**, *47*, 259–264.

(28) Yoshida, S. *Chem. Pharm. Bull.* **1963**, *11*, 628–638.

(29) Delgado, M. J. M.; Marquez, F.; Suero, M. I.; Marcos, J. I. *Spectrosc. Lett.* **1988**, *21*, 841–852.

(30) Akyuz, S. *J. Mol. Struct.* **2003**, *651*, 541–545.

(31) Lautie, A.; Froment, F.; Novak, A. *Spectrosc. Lett.* **1976**, *9*, 289–299.

(32) Desiraju, G. R.; Steiner, T. *The Weak Hydrogen Bond in Structural Chemistry and Biology*; Oxford University Press: Oxford, 1999.

(33) Kawakami, K. *J. Pharm. Sci.* **2007**, *96*, 982–989.

(34) Kawakami, K.; Ida, Y. *Thermochim. Acta* **2005**, *427*, 93–99.

(35) Nishimori, A.; Sorai, M. *J. Phys. Chem. Solids* **1999**, *60*, 895–904.

(36) Burger, A.; Ramberger, R. *Microchim. Acta* **1979**, *2*, 259–271.

(37) Burger, A.; Ramberger, R. *Microchim. Acta* **1979**, *2*, 273–316.

(38) Wirth, D. D.; Stephenson, G. A. *Org. Process Res. Dev.* **1997**, *1*, 55–60.